Smoothed Particle Hydrodynamics Simulation for Continuous Casting

A D I T H Y A V I J A Y K U M A R

Master of Science Thesis
Stockholm, Sweden 2012

Smoothed Particle Hydrodynamics Simulation for Continuous Casting

A D I T H Y A V I J A Y K U M A R

Master's Thesis in Scientific Computing (30 ECTS credits)
Master Programme in Scientific Computing, 120 credits
Royal Institute of Technology year 2012
Supervisor at KTH was Jesper Oppelstrup
Examiner was Michael Hanke

TRITA-MAT-E 2012:11
ISRN-KTH/MAT/E--12/11--SE

Royal Institute of Technology
School of Engineering Sciences

KTH SCI
SE-100 44 Stockholm, Sweden

URL: www.kth.se/sci

Abstract

Smoothed Particle Hydrodynamics Simulation for Continuous Casting

This thesis proposes a way of simulating the continuous casting process of steel using Smoothed Particle Hydrodynamics(SPH). It deals with the SPH modeling of mass, momentum and the energy equations. The interpolation kernel functions required for the SPH modeling of these equations are calculated. Solidification is modeled by some particles are used to represent fluids and others solids. Elastic forces are calculated between the particle neighbors to create deformable bodies. The fluid solidifies into the elastic body when it cools down and the elastic body melts as it is heated. In continuous casting the molten metal solidifies forming a shell when it comes in contact with the cold wall. The mold of the continuous casting is modeled with a cold oscillating wall and a symmetric wall. Once the shell is formed water is sprayed on the solidified metal. If the shell is thin and cooling is not sufficient, the elastic body melts due to the effect of the hot fluid.

Sammanfattning

Stränggjutningssimulering med Smoothed Particle Hydrodynamics

Den klassiska SPH-modellen för vätskor med fri yta kompletteras med värmeledning med fasomvandling och stelning: partiklar kan byta mellan vätske-tillstånd och solid-tillstånd beroende på temperaturen. Elastiska krafter beroende på avstånd mellan partiklarna aktiveras i solid-tillståndet och slås av i fluid-tillstånd så att vätskan kan stelna och senare smälta igen om så behövs. Vid stränggjutning stelnar smältan, som fylls på via ett rör, vid kontakt med en oscillerande, kall kokill-vägg, till ett elastiskt skal. Detta kyls fortlöpande genom påsprutning av vatten utanpå kokillen och direkt på skalet, som förångas. Skalet deformeras nedanför kokillen av det hydrostatiska trycket från smältan; om det är för tunt brister det. Som demonstration gjordes en simulering där ett skal skapas, varpå man slår av vattenkylningen på ett parti: då smälter skalet och blir tunnare och till sist brister det och all smälta rinner ut genom hålet. Noggrannheten i simuleringen lämnar en del att önska men det vore mycket svårt att bygga en så komplex modell med vanlig CFD.

Acknowledgements

I am extremely grateful to Prof. Dr. Jesper Oppelstrup for being my mentor. He has helped me at various stages during my master thesis which includes providing me with a well defined problem equipping me with the necessary tools and techniques and willingly sharing his knowledge and ideas with me.

I would like to thank my friend Navaladi Arichunan, with whom I have enjoyed numerous scientific and non-scientific discussions.

Thanks to Manual Baumann and Slobodan Milovanovic, with whom I did a project that led to the thesis.

I would like to thank my family in India for their support and encouragement.

Finally, I would like to thank Dr. Michal Hanke for giving me some extra time to complete this report.

Contents

List of Figures

To my family and friends

Chapter 1

Introduction

1.1 Continuous Casting

The continuous casting process is illustrated in Fig. 1.1. In the process molten metal is solidified into a "semifinished" billet, bloom, or slab for subsequent rolling in the finishing mills. The focus in this work is on continuous casting of steel, in a machine where the solidifying strand is cooled by water spray while bent by the roller system from vertical to horizontal. To give an idea of the size of the machinery, the radius of curvature is O(10 m) and the cross section of the strand is about 1 metre times one to six metre. The metal is supplied trough the Submerged Entry Nozzle a foot or so below the liquid pool surface (called the Meniscus) which is covered by several cm of mold flux powder as thermal insulation. The composition of the mold flux powder is important for the surface properties of the slab. The Mold has water cooling channels, and there is a millimetre-thin sheet of molten mold flux as lubrication between the solidifying steel shell and the mold. The mold oscillates vertically with cm-amplitude at a few Hz. The casting parameters, like casting speed, angles of mold walls, oscillations of mold, and mold flux powder, all influence the quality of the slabs and the stability of the process. It may happen that the shell sticks to the mold at some point, which makes a surface defect, or at worst may lead to breaking of the shell below the mold. Such break-outs are very costly; after the introduction of the a ceramic stopper in the ladle, the amount of steel lost in a breakout is limited to the volume of the tundish.

Simulation models have been built with different levels of fidelity, from CON1D which treats 1D heat transfer from liquid steel through solid shell, mold flux and its associated potential gas gaps, and mold or water spray. The next level of fidelity, CON2D, is offered by modeling a horizontal cut traveling with the cast downwards. Such a model

can provide approximations to the mechanical stresses in the solid shell and can shed light on what happens at the corners.

However, none of these models treat the flow of the melt accurately, and the stress predictions have to make assumptions about the z-direction. Current high-fidelity simulation models run 3D CFD of turbulent flow from the SEN, with a free surface meniscus with a layer of melting mold flux powder, and some approximation to a proper model for stresses and strains in the shell. However, high-fidelity treatment of the flow and solid has not yet been demonstrated. Such simulations must be time-accurate to account for mold oscillations and the waves appearing on the meniscus.

A steady-state model for 2D plane and axi-symmetric caster was developed by KIMAB, and Fig. 1.2 shows a simulation prediction. Note that the thickness of the slag film varies along the mold as required by force equilibrium between the hydrodynamic lubrication forces in the thin film and the liquid metal pressure not balanced by the solid shell stresses. The shell is only about 1 cm thick as it leaves the mold.

The numerical models are quite sensitive and much effort has been spent on making them robust enough to provide guidance in parameter choice, but with limited success. The present work makes an attempt to use particle models instead. It is usually relatively easy to include detailed physics modeling at the expense of computer time because they represent all temporal scales.

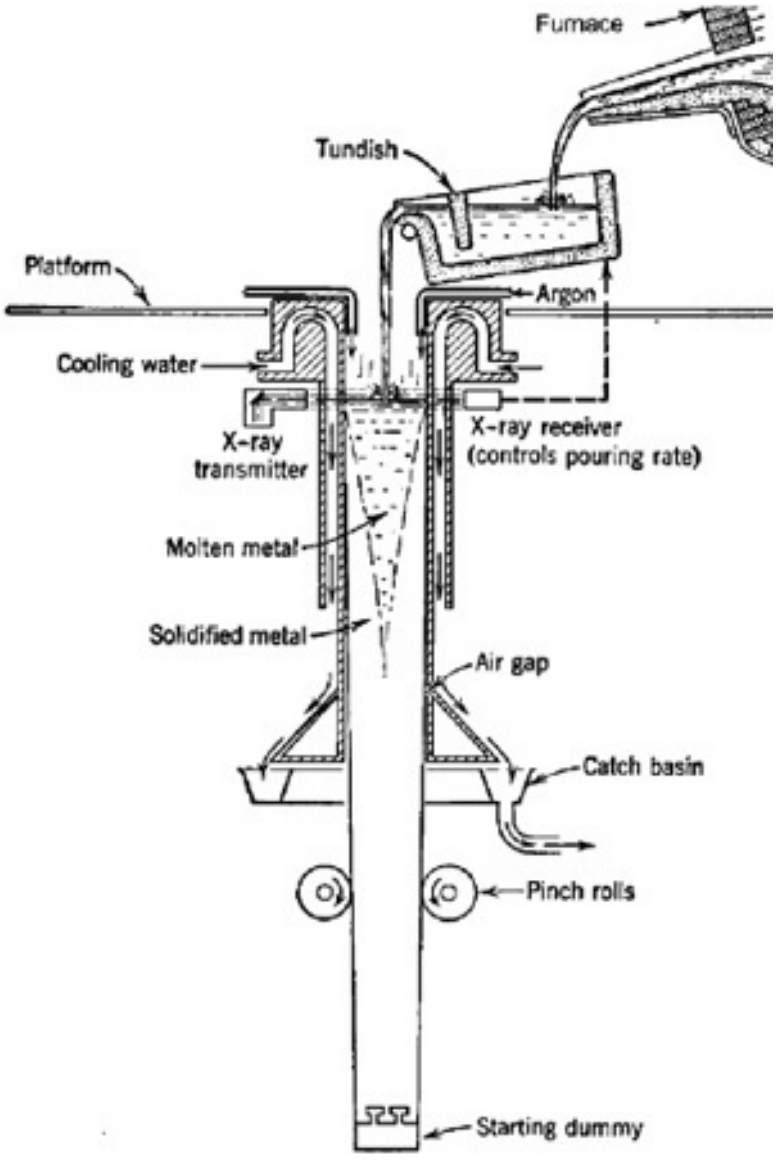

FIGURE 1.1: Vertical Casting Process (form Continuous Casting Consortium)

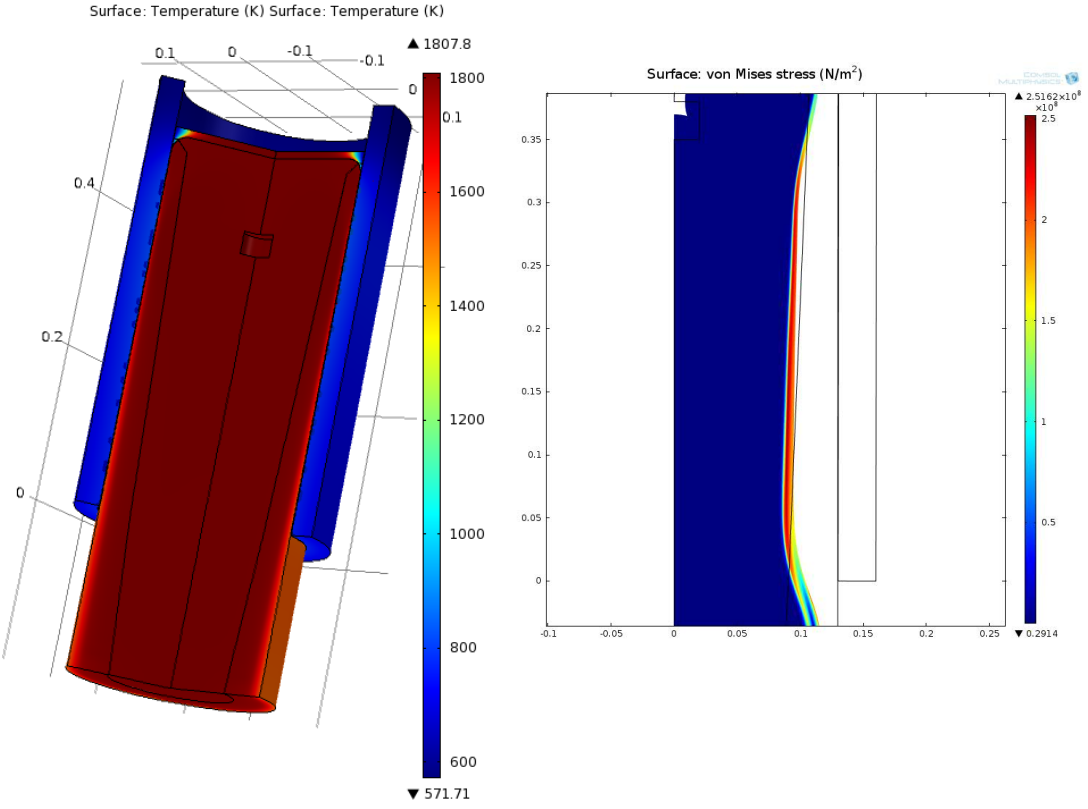

FIGURE 1.2: Left, axi-symmetric model, right, deformation of solid shell

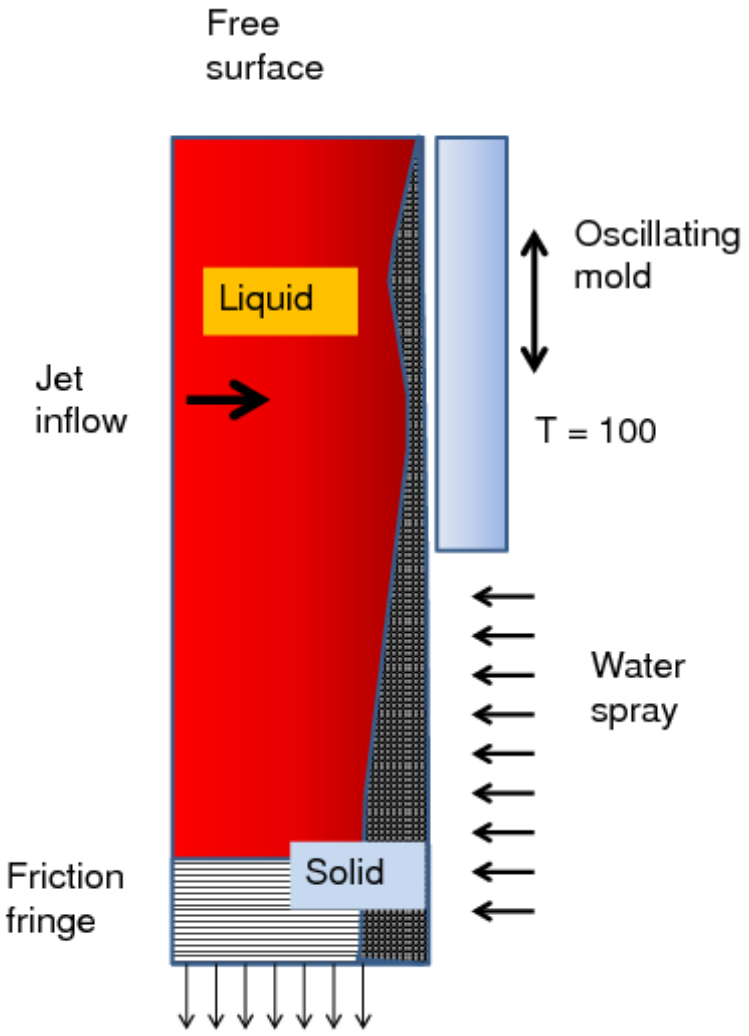

FIGURE 1.3: Sketch of SPH simulation model

In this thesis an attempt has been made to simulate a vertical continuous casting process of steel, see Fig. 1.3 The setup consists of a reservoir for the melt, from which it is poured into the mold. The left boundary is a symmetry boundary. The cold mold wall oscillates up and down to enable better solidification. The mold is made up of copper and is cooled by water channels, simulated by keeping its temperature at 100C on the outside. Below the mold, the solidified shell is cooled by water spray. The outflow is proportional to the pressure head, with a ratio chosen to give the desired casting speed and meniscus height. The simulation reaches a quasi-steady state for the free surface location.

1.2 Smoothed Particle Hydrodynamics

Smoothed particle hydrodynamics (SPH) belongs to the class of Lagrangian approaches to fluid simulation. In simulations based on the Lagrangian approach, fluids are represented by a set of particles. SPH allows one to compute the value of any variable, such as density, at arbitrary positions in the fluid by smoothing over the set of all nearby particles. Euler simulations, on the other hand, use a fixed grid instead of particles.

1.2.1 Governing Equations of Fluids

The Navier-Stokes Equation for an incompressible fluid is given by:

$$\rho\frac{D\vec{u}}{Dt} = -\nabla p + \mu\nabla.(\nabla\vec{u}) + \vec{f} \quad (1.1)$$

$$\nabla.\vec{u} = 0 \quad (1.2)$$

where ρ is the density field of the fluid, $\vec{u}$ the velocity field, p the pressure field, t is time, μ the dynamic viscosity, and $\vec{f}$ is the sum of internal and external force density fields. The material derivative expresses the time rate of change for a material point which follows the velocity field,

$$\frac{D}{Dt} \equiv \frac{\partial}{\partial t} + \vec{u}\cdot\nabla$$

The convective term, $\vec{u}\cdot\nabla\vec{u}$, is needed in Eulerian simulations which describe the process at fixed points in space In SPH, however, the particles move with the fluid, so the material derivative equals the time rate of change. As the mass of particles is constant in this SPH simulation the mass conservation is automatic. The Lagrangian formulation of the Navier-Stokes equation is:

$$\rho\frac{d\vec{u}}{dt} = -\nabla p + \mu\nabla.(\nabla\vec{u}) + \vec{f} \quad (1.3)$$

$\mu\nabla^2\vec{u}$ is the viscosity term, which has a smoothing effect on the velocity field of the fluid. ∇p is the force per unit volume that is due to pressure, which causes the particles to get away from locations of high pressure.

In (1.3) the right hand side can be considered as the total force per unit volume (F), the sum of internal F_{int} and external F_{ext} forces. Hence (1.3) can be rewritten as:

$$\begin{aligned} \rho \frac{d\vec{u}}{dt} &= F \\ \frac{m}{V}\frac{d\vec{u}}{dt} &= F \\ \bar{F} &= m\vec{a} \end{aligned} \tag{1.4}$$

where $\bar{F} = FV$ the total force.

Hence the basic idea used in SPH is Newtons second law of motion.

The pressure law used in here is:

$$p = \frac{{c_s}^2 \rho_0}{\gamma}\left[\left(\frac{\rho}{\rho_0}\right)^{\gamma} - 1\right] \tag{1.5}$$

where c_s is the speed of sound, ρ_0 is the reference density, ρ is the density, γ depends on the material used (molten metals = 7)

1.2.2 Smoothing Values

SPH is an interpolation method to approximate values and derivatives of continuous field quantities by using discrete sample points. Sampled points are called smoothed particles, and they carry concrete entities, e.g. mass, velocity, and position. Particles also can carry estimated physical field quantities dependent on the problem, e.g. temperature, enthalpy, and pressure. SPH quantities are macroscopic and are obtained as weighted averages from the adjacent particles. SPH can approximate the derivatives of continuous fields using analytical differentiation on particles located completely arbitrarily.

To find the value of the scalar field $A(\vec{r})$ at any point, the following formula is used [1]:

$$A(\vec{r}) = \sum_j A_j V_j W(\vec{r} - \vec{r_j}, h) \tag{1.6}$$

where the subscript j iterates over all particles, $\vec{r_j}$ is the current position of particle j, V_j is the volume of the particle and h is the support radius of the Kernel Function, see below.

The gradient of the scalar field is given by:

$$\nabla A(\vec{r_i}) = \sum_j A_j V_j \nabla W(\vec{r_i} - \vec{r_j}, h) \tag{1.7}$$

and the laplacian is :

$$\nabla^2 A(\vec{r_i}) = \sum_j A_j V_j \nabla^2 W(\vec{r_i} - \vec{r_j}, h) \tag{1.8}$$

since the product $A_j V_j$ does not depend on any component of space.

1.2.3 Smoothing Kernels

Smoothing Kernels $W(., h)$ can be compared to different schemes in Finite Difference Method and hence they are of significant importance. The length scale of W is h. Usually, and for all kernels used in this work, W has compact support. The properties are [1]:

$$\int_\Omega W(\vec{r}, h) d\vec{r} = 1 \tag{1.9}$$

$$W(\vec{r}, h) = 0, ||\vec{r}|| \geq h, \tag{1.10}$$

$$\lim_{h \to 0} W(\vec{r}, h) = \delta(\vec{r}) \tag{1.11}$$

where δ is the Dirac delta "function":

$$\delta(\vec{r}) = \begin{cases} \infty & ||r|| = 0 \\ 0 & otherwise \end{cases} \tag{1.12}$$

The unit integral ensures that maxima and minima are not enhanced. In this thesis a total of four types of smoothing kernels is used: the default polynomial kernel (W_{poly}) used for the calculation of density and temperature, the spiky kernel (W_{spiky}) used for the calculation of pressure forces, the viscosity kernel (W_{visc}) used for the calculation of viscous forces and the sine kernel (W_{sine}) used for the calculation of elastic forces. These kernel function are explained in detail in Chapter 2

Chapter 2

Density and Forces

2.1 Mass Density

In Chapter 1 it was explained that a continuous quantity field, their gradients, or Laplacians can be approximated by using the SPH formulations (1.6), (1.7). (1.8) To apply these equations the particle masses and mass densities must be known. The particle mass is defined by the user before the simulation is started and remains a constant, but the mass-density is a continuous field of the fluid, which must be computed. (1.6) can be used to computhe the mass density.

$$\begin{aligned} \rho = \rho(\vec{r_i}) &= \sum_j \rho_j \frac{m_j}{\rho_j} W_{poly}(\vec{r_i} - \vec{r_j}, h) \\ &= \sum_j m_j W(\vec{r_i} - \vec{r_j}, h) \end{aligned} \tag{2.1}$$

2.2 Internal Forces

These are the forces from within a fluid. The pressure and viscous forces are the internal forces.

2.2.1 Pressure Force

The pressure force at a particle i in terms of SPH notation is given by:

$$\begin{aligned} f_i^{pressure} &= -\nabla p(r_i) \\ &= -\sum_{j \neq i} p_j \frac{m_j}{\rho_j} \nabla W_{spiky}(\vec{r_i} - \vec{r_j}, h) \end{aligned} \tag{2.2}$$

The pressure force in 2.2 is not symmetrical. This is because when two particle interact the first uses only the pressure of the second particle to calculate its pressure force and vice versa. [2] gives a simple solution to symmetrize the pressure forces, that is best suited for speed and stability:

$$f_i^{prssure} = -\sum_{i \neq j} \frac{p_i + p_j}{2} \frac{m_j}{\rho_j} \nabla W_{spiky}(\vec{r_i} - \vec{r_j}, h) \tag{2.3}$$

At places where the mass density is balanced by the reference density the pressure forces are zero. In regions where the mass density is very high the pressure forces produced will be repulsive as the particles must move away from each other to achieve the reference density. In regions with low mass density the pressure forces will be attractive as the particles must move toward one another. The pressure is calculated using 1.5. The kernel function used to calculate the pressure forces is different from the one used to calculate density. From 2.3 we see that for the calculation of the pressure force the gradient of the kernel function is needed. If we were to use the W_{poly} kernel particle clustering will arise in high pressure regions. This is because $\nabla W_{poly}(\vec{r}, h) \rightarrow 0$ then $||\vec{r}|| \rightarrow 0$, which implies that the repulsion forces attenuate as the particles approach each other. Hence the gradient of the kernel function mus not be zero when the particles are close to each other. For the pressure force calculation the *spiky* kernel suggested by [2] is used.

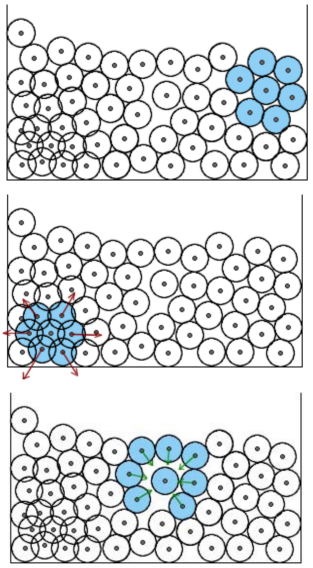

FIGURE 2.1: Positive, Negative and Zero Pressure Forces

2.2.2 Viscous Forces

A fluid is a substance that cannot resist shear stress and consequently will flow upon deformation. At the same time when the fluid flows, the molecules undergo internal friction that will decrease its kinetic energy by converting it into heat. Resistance to flow is called viscosity, and the viscosity coefficient, μ , defines the strength of how viscous the fluid is.

The viscous force at a particle i in terms of SPH notation is given by:

$$\begin{aligned} f_i^{viscous} &= \mu \nabla^2 \vec{u}(\vec{r_i}) \\ &= \mu \sum_{j \neq i} \vec{u_j} \frac{m_j}{\rho_j} \nabla^2 W_{visc}(\vec{r_i} - \vec{r_j}, h) \end{aligned} \tag{2.4}$$

Like the pressure forces the viscous forces in 2.4 are not symmetric as the velocity varies from particle to particle. To symmetrize this viscous forces are calculated using the formula suggested by [2]:

$$\begin{aligned} f_i{}^{viscous} &= \mu \sum_{i \neq j} (\vec{u_j} - \vec{u_i}) \frac{m_j}{\rho_j} \nabla^2 W_{visc}(\vec{r_i} - \vec{r_j}, h) \\ &= \mu \sum_{i \neq j} (\vec{u_j} - \vec{u_i}) \frac{m_j}{\rho_j} W^{"}_{visc}(\vec{r_i} - \vec{r_j}, h) \end{aligned} \tag{2.5}$$

The kernel function used for the viscous force calculation must have its gradient positive. This is required for the system to be dissipative, i.e. the forces forces due to viscosity must not increase the relative velocity, and thereby introduce energy and instability into the system. If the Laplacian is positive everywhere only then will the viscosity force work as a damping term, and damp the relative velocity. The standard kernel does not have this property and neither does the pressure kernel. Hence a new kernel must be introduced where $\nabla^2 W_{visc}(\vec{r}, h) \geq 0$ then $\vec{r} \leq h$. The kernel proposed by [2] is used for viscous force calculations.

2.3 External Forces

The external forces are balanced by the internal force. The external force include gravity, surface tension and elastic forces(in the solidified part).

2.3.1 Gravity

The gravitational force density field is acting equally on all fluid particles, and on a particle i is given by:

$$f_i^{gravity} = \rho_i \vec{g} \tag{2.6}$$

where $\vec{g}$ is the acceleration due to gravity.

2.3.2 Surface Tension

Cohesive forces exist between fluid molecules, and this allows it to resist external forces. When compared to a submerged particle, on which the forces due to other particles are equal in all directions, the particles at the surface have unbalanced forces, and this results in surface tension. The direction of the surface tension force is always in the direction of the inward surface normal towards the fluid

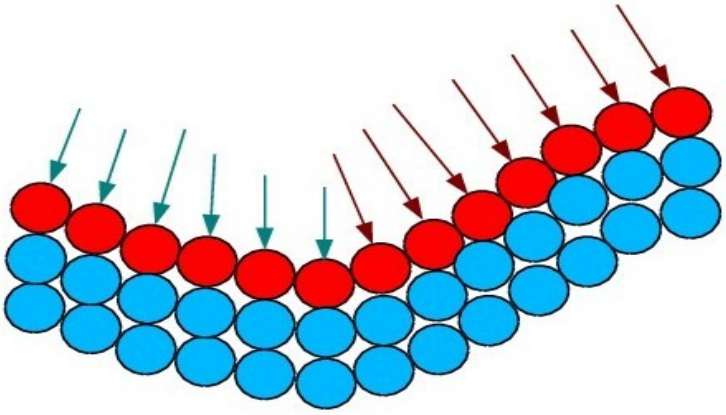

FIGURE 2.2: Surface Tension Forces

2.2 shows that when the curvature at the surface is positive then the surface tension force is larger(red arrows), when compared if the curvature was negative(blue arrow).

The surface of the fluid can be found using a color field, which in SPH notation is given by [2]:

$$c_s(\vec{r}) = \sum_j \frac{m_j}{\rho_j} W_{poly}(\vec{r_i} - \vec{r_j}, h) \tag{2.7}$$

The gradient of the color field:

$$\mathbf{n} = \nabla c_s \tag{2.8}$$

gives the surface normal. This surface normal points into the fluid.

The divergence of the surface normal gives the curvature of the surface:

$$\kappa = \frac{-\nabla^2 c_s}{|\mathbf{n}|} \tag{2.9}$$

The surface tension force is given by [2]

$$f_i^{surface} = -\sigma \nabla^2 c_s \frac{\mathbf{n}}{|\mathbf{n}|} \tag{2.10}$$

where σ is a co-efficient depending on the fluid.

2.4 Smoothing Kernels

As discussed in the previous section three different kernels are used to calculate the density, pressure force and the viscous force. This section describes the derivation and properties of each kernel function. The kernel used in [2] is a 3D kernel. As the simulation here is in 2D the kernel functions for 2D is derived.

2.4.1 The Polynomial Kernel

The Polynomial Kernel suggested by [2] is the default kernel used for the calculation of density, surface tension force and in temperature modeling. It is given by:

$$W_{poly}(\vec{r}, h) = A \begin{cases} (h^2 - ||r||^2)^3 & 0 \leq ||\vec{r}|| \leq h \\ 0 & ||\vec{r}|| > h \end{cases} \tag{2.11}$$

Where A can be found out using the condition:

$$\int_\Omega W_{poly} d\Omega = 1 \tag{2.12}$$

We find A to be:

$$\begin{aligned} A &= \frac{315}{64\pi h^9} \quad 3D \\ A &= \frac{4}{\pi h^8} \quad 2D \end{aligned} \tag{2.13}$$

From W the gradient and laplacians can be calculated

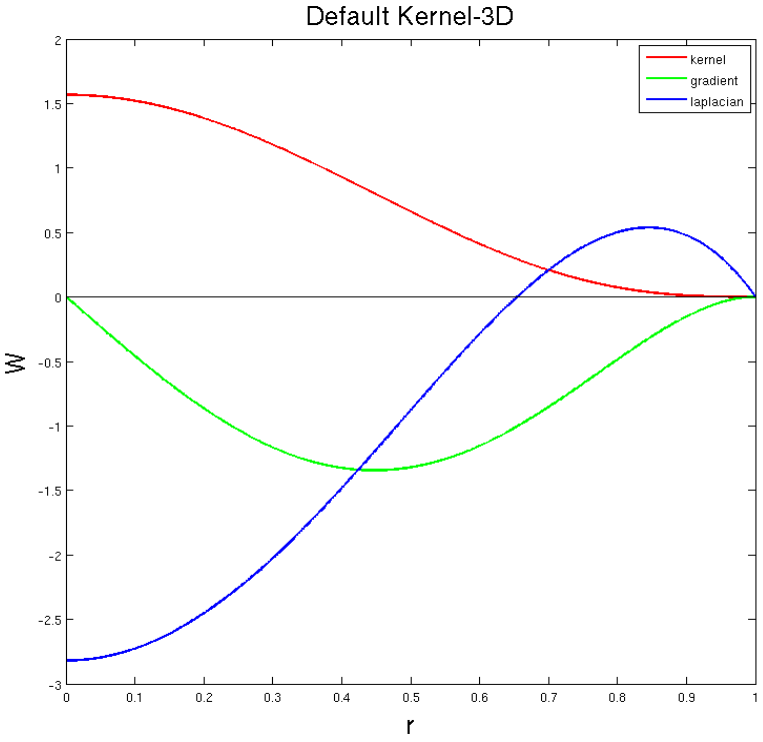

FIGURE 2.3: Polynomial Kernel, its Gradient and Laplacian

$$\begin{aligned} \nabla W_{poly} &= -B.\vec{r}(h^2 - ||r^2||)^2 \\ B &= \frac{945}{32\pi h^9} \quad 3D \\ B &= \frac{24}{\pi h^8} \quad 2D \end{aligned} \tag{2.14}$$

$$\begin{aligned} \nabla^2 W_{poly} &= -C.(h^2 - ||r^2||)(3h^2 - 7||r^2||) \\ C &= \frac{945}{32\pi h^9} \quad 3D \\ C &= \frac{24}{\pi h^8} \quad 2D \end{aligned} \tag{2.15}$$

From 2.3 we can see that the polynomial kernel preserves the properties of the Gaussian bell curve.

2.4.2 The Spiky Kernel

For the calculation of the pressure force the gradient of the kernel function is needed. If we were to use the polynomial kernel, then from 2.3 we see that as the distance between the particle reduces the value of the gradient of the kernel becomes zero making the pressure force zero. This leads to the particles to overlap as the repulsive force is very low. This is the reason a different kernel has to be used to find the pressure force. The kernel suggested by [2] is :

$$W_{spiky}(\vec{r},h) = A \begin{cases} (h-||r||)^3 & 0 \leq ||\vec{r}|| \leq h \\ 0 & ||\vec{r}|| > h \end{cases} \tag{2.16}$$

Where A can be found out using the condition:

$$\int_{\Omega} W_{spiky} d\Omega = 1 \tag{2.17}$$

We find A to be:

$$\begin{aligned} A &= \frac{15}{\pi h^6} \quad 3D \\ A &= \frac{10}{\pi h^5} \quad 2D \end{aligned} \tag{2.18}$$

From W the gradient and laplacians can be calculated

$$\begin{aligned} \nabla W_{spiky} &= -B.\frac{\vec{r}}{||\vec{r}||}(h-||r||)^2 \\ B &= \frac{45}{\pi h^6} \quad 3D \\ B &= \frac{30}{\pi h^5} \quad 2D \end{aligned} \tag{2.19}$$

$$\begin{aligned} \nabla^2 W_{spiky} &= -C.(h-||r||)(h-2||r||)/||\vec{r}|| \\ C &= \frac{90}{\pi h^6} \quad 3D \\ C &= \frac{60}{\pi h^5} \quad 2D \end{aligned} \tag{2.20}$$

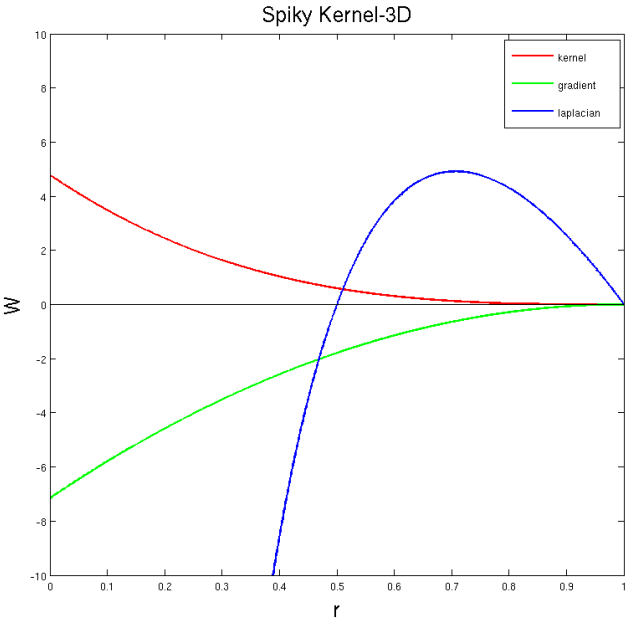

FIGURE 2.4: Spiky Kernel, its Gradient and Laplacian

2.4.3 The Viscosity Kernel

For the calculation of the viscous force the laplacian of the kernel function is needed. If we were to use the polynomial kernel, then from 2.3 we see that the laplacian of the polynomial function is negative and this increases the velocities due to the relative velocity and thereby introduce energy and instabilities to the system. For the system to be dissipative the kernel suggested by [2] is used:

$$W_{visc}(\vec{r},h) = A \begin{cases} -\frac{||r||^3}{2h^3} + \frac{||r||^2}{h^2} + \frac{h}{2||r||} - 1 & 0 \leq ||\vec{r}|| \leq h \\ 0 & ||\vec{r}|| > h \end{cases} \tag{2.21}$$

Where A can be found out using the condition:

$$\int_\Omega W_{visc} d\Omega = 1 \tag{2.22}$$

We find A to be:

$$\begin{aligned} A &= \frac{15}{2\pi h^3} \quad 3D \\ A &= \frac{10}{3\pi h^2} \quad 2D \end{aligned} \tag{2.23}$$

From W the gradient and laplacians can be calculated

$$\begin{aligned} \nabla W_{visc} &= -B.\vec{r}(\frac{-3||\vec{r}||}{2h^3} + \frac{2}{h^2} - \frac{h}{2||\vec{r}||^3}) \\ B &= \frac{15}{2\pi h^3} \quad 3D \\ B &= \frac{10}{\pi h^2} \quad 2D \end{aligned} \tag{2.24}$$

$$\begin{aligned} \nabla^2 W_{visc} &= -C.(h - ||r||) \\ C &= \frac{45}{2\pi h^6} \quad 3D \\ C &= \frac{20}{\pi h^5} \quad 2D \end{aligned} \tag{2.25}$$

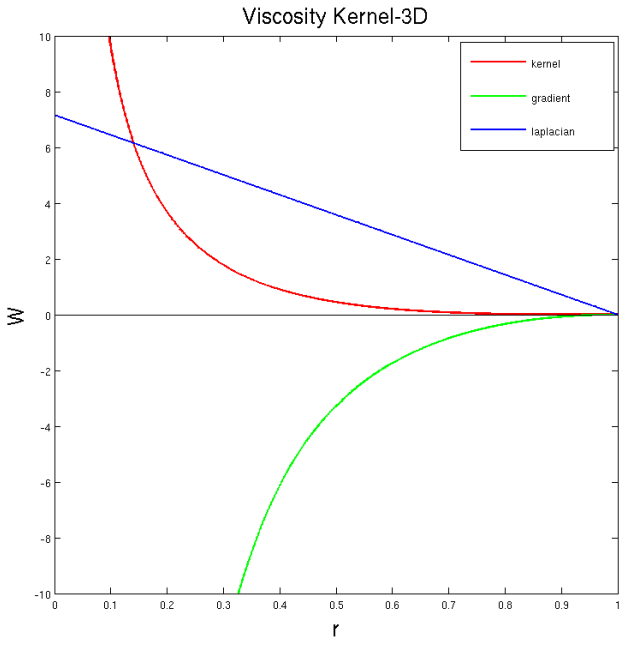

FIGURE 2.5: Viscosity Kernel, its Gradient and Laplacian

Chapter 3

Modeling the Energy Equation

3.1 Euler's Energy Equation

Eulers Energy equation is given by:

$$\frac{\partial e}{\partial t} + \nabla.(e+p)\mathbf{v} = 0 \tag{3.1}$$

where e is the energy, p the pressure and $\mathbf{v}$ the velocity. As in this thesis prominence is given to the solidification process, an appropriate method to model the energy equation is to use an entalpy formulation.

[3] suggests a way of modelling the energy equation by calculation the Enthalpy and later the temperature.

3.1.1 SPH model of the Energy Equation

The SPH Energy Equation for a particle i and its neighbor j is given by:

$$\frac{dH_i}{dt} = \sum_j \frac{4m_j}{\rho_i \rho_j} \frac{\kappa_i \kappa_j}{\kappa_i + \kappa_j} T_{ij} \frac{\mathbf{r_{ij}}.\nabla W_{ij}^{poly}(\mathbf{r_{ij}}, h)}{\mathbf{r_{ij}^2}} \tag{3.2}$$

At the beginning of the simulation the temperature of each particle is specified. Using this the Enthalpy is calculated using 3.2. In the next time step the the temperature is evaluated from the fitted data as shown in 3.1

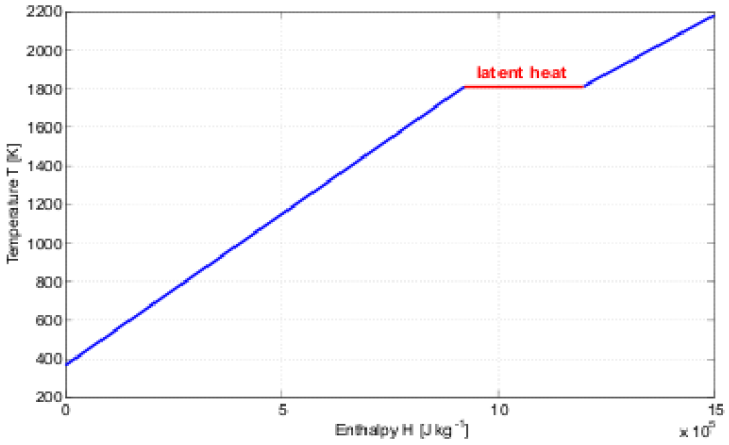

FIGURE 3.1: Mapping of Temperature from Enthalpy

3.1.2 Validation of the Temperature Model

The SPH simulation of a benchmark problem was compared with the well-known fundamental solution of heat equation. For this the particles are arranged in a regular grid and all the external and internal forces are turned off. An initial gaussian temperature setting is done so that the temperature is maximum at the centre of the grid and and decreases based on the gaussian function. With time the temperature spreads out.

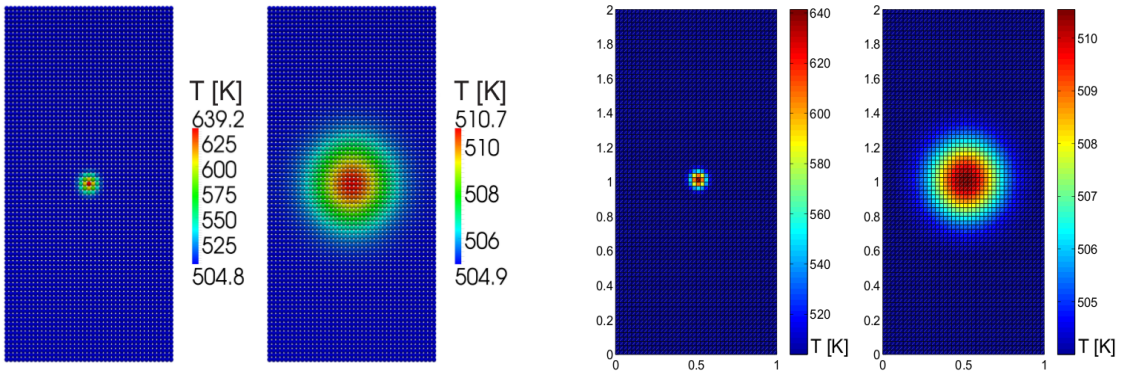

FIGURE 3.2: Numerical Test Calculation

Fig.3.2 shows that the results obtained from the simulation matches with the fundamental solution. The first two figures show the particle simulation during time t = 0s and t = 5s. The third((t = 0s) and fourth (t = 5s) figures is the fundamental solution of the heat equation calculated in matlab. The results obtained form the particle simulation agrees with the matlab solution.

3.1.3 Test Case - Dam Break Problem

In order to test the temperature model, a dam break simulation is considered. Initially the fluid particles are arranged in a regular grid. The temperatre of the fluid particles is maintained at 2000 units. The right wall is kept at a cooler temperature (1500 units). When the simulation begins the regular grid of fluid particles collapses due to gravity and hits the cold wall. At this point we can see the heat transfer from the hot liquid to the cold wall.

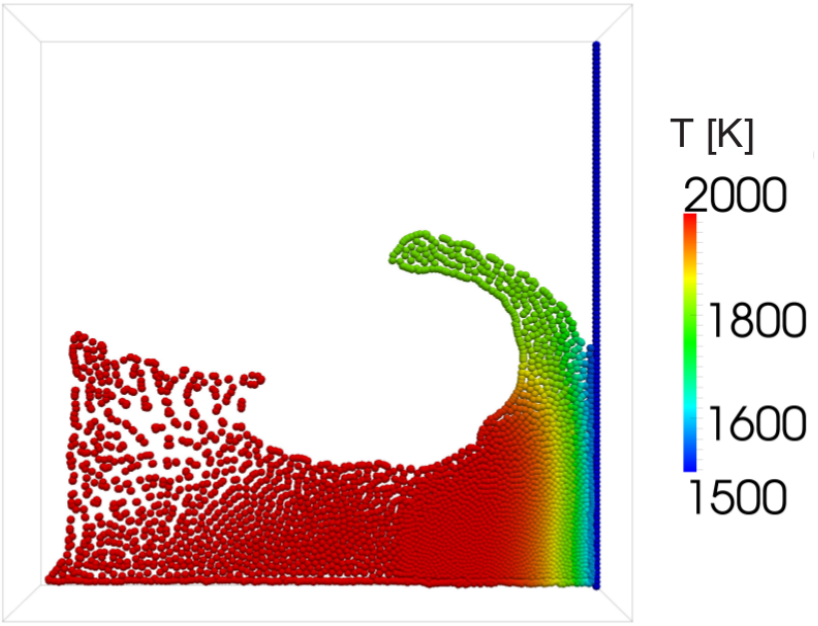

FIGURE 3.3: Dam Break with a cold wall

Fig.3.3 clearly shows the heat transfer occurring between the cold wall and the hot fluid.

Chapter 4

Solidification using Smoothed Particle Hydrodynamics

This section deals with the solidification of the molten metal to form an elastic body and the fluid-solid interactions. Whenever the temperature of a particle drops below a threshold associated with the material, it joins a nearby object or forms an elastic body with its cold neighbors.

4.1 Theory of Elasticity

An elastic body is one which returns to its original configuration when the deforming forces are removed. In this section it is assumed that the material is *perfectly elastic*, i.e. the material assumes its initial form completely after the removal of the deforming forces. Also the elastic bodies are assumed to be *homogeneous*, i.e. the smallest element cut from the body will possess the same properties as the body. Also the body is assumed to be *isotropic*, i.e. elastic properties are same in all directions.

4.1.1 Stress

When a body is in equilibrium under the action of external forces, internal forces will be formed between the parts of the body. To find the magnitude of these forces at any point, a cross section at this point is considered. This divides the body into two parts, and one of these parts can be considered to be in equilibrium under the action of external forces and internal forces, that represents the action of the other part on this part. The internal forces act like hydrostatic pressure, i.e. continuously distributes

over the area. The intensity of the internal forces is called as *stress*. Stress can be expressed as a second-order tensor, with nine components of which six are independent components.

$$\boldsymbol{\sigma} = \begin{bmatrix} \sigma_{xx} & \sigma_{xy} & \sigma_{xz} \\ \sigma_{yx} & \sigma_{yy} & \sigma_{yz} \\ \sigma_{zx} & \sigma_{zy} & \sigma_{zz} \end{bmatrix} \tag{4.1}$$

4.1.2 Strain

When deformation of the elastic body is considered, it is assumed that there are enough constraints to prevent rigid body motion, so that motion of particles is not possible without deformation. This deformation is measured by the strain tensor. This is also a rank two tensor with nine components of which six are independent.

$$\boldsymbol{\epsilon} = \begin{bmatrix} \epsilon_{xx} & \epsilon_{xy} & \epsilon_{xz} \\ \epsilon_{yx} & \epsilon_{yy} & \epsilon_{yz} \\ \epsilon_{zx} & \epsilon_{zy} & \epsilon_{zz} \end{bmatrix} \tag{4.2}$$

According to [4] the Green-Saint-Venant strain is given by

$$\epsilon = \frac{1}{2}(\nabla \mathbf{u} + \nabla \mathbf{u}^{\mathbf{T}} + \nabla \mathbf{u} \nabla \mathbf{u}^{\mathbf{T}}) \tag{4.3}$$

4.1.3 Hooke's Law

The relation between the components of stress and strain are established experimentally and are known as *Hooke's Law*. This law states that "the stress is directly proportional to the strain in the elastic region".

$$\boldsymbol{\sigma} = \boldsymbol{C}\boldsymbol{\epsilon} \tag{4.4}$$

C is a fourth rank tensor with 81 components. But as the material is isotropic and homogeneous, we have 36 components with 21 independent components.

$$\begin{bmatrix} \sigma_{xx} \\ \sigma_{yy} \\ \sigma_{zz} \\ \sigma_{xy} \\ \sigma_{yz} \\ \sigma_{zx} \end{bmatrix} = \frac{E}{(1+\nu)(1-2\nu)} \begin{bmatrix} 1-\nu & \nu & \nu & 0 & 0 & 0 \\ \nu & 1-\nu & \nu & 0 & 0 & 0 \\ \nu & \nu & 1-\nu & 0 & 0 & 0 \\ 0 & 0 & 0 & 1-2\nu & 0 & 0 \\ 0 & 0 & 0 & 0 & 1-2\nu & 0 \\ 0 & 0 & 0 & 0 & 0 & 1-2\nu \end{bmatrix} \begin{bmatrix} \epsilon_{xx} \\ \epsilon_{yy} \\ \epsilon_{zz} \\ \epsilon_{xy} \\ \epsilon_{yz} \\ \epsilon_{zx} \end{bmatrix} \tag{4.5}$$

4.2 Displacement and its gradient

The solidification of fluid to an elastic body explained in this chapter is based on the approach by [5]. At the position of every particle, the gradient of displacement from the original shape of the body is estimated, then the gradient is used to compute the strain and stress tensors.

The difference of displacement of a pair of particles i and j in the same elastic body is given by:

$$\mathbf{u_{ij}} = \mathbf{u_j} - \mathbf{u_i} = \mathbf{r_j} - \mathbf{r_i} + \mathbf{x_{ij}} \tag{4.6}$$

Where $\mathbf{x_{ij}}$ is the vector between the two particles at the time of freezing. By definition we have

$$A = \sum_j A_j v_j W(\mathbf{x_{ij}}, h) \tag{4.7}$$

and

$$\nabla A = \sum_j A_j v_j \nabla W(\mathbf{x_{ij}}, h) \tag{4.8}$$

Hence for displacement we can write :

$$\nabla \mathbf{u} = \sum_j \bar{v_j} \nabla W(\mathbf{x_{ij}}, h)(\mathbf{u_j} - \mathbf{u_i})^T \tag{4.9}$$

where $\bar{v_j}$ is the body volume(volume at the time of freezing) of particle j. Here $\mathbf{u_j} - \mathbf{u_i}$ is used instead of $\mathbf{u_j}$ because of the way SPH behaves at the border of particle samples.If the object were translated in the positive direction of u, the gradient would point inwards, while it would point out of the object after translations into the negative direction of u.The use of the difference of displacement cancels this effect, while at the same time

making sure that the length of the gradient at the border of an object stays the same if the object is translated without further deformation.

The derivative of 4.9 w.r.t. $\mathbf{u_j}$ is:

$$\mathbf{d_{ij}} = \frac{\partial \nabla \mathbf{u}}{\partial \mathbf{u_j}} = \bar{v}_j \nabla W(\mathbf{x_{ij}}, h) \tag{4.10}$$

4.3 Strain Energy and the Elastic Force

The elastic force is defined as the negative gradient of the strain energy, U, with respect to the displacement:

$$F^{(ji)}_{Elastic} = -\nabla_{\mathbf{u}_j} U^{(i)} \tag{4.11}$$

Where $F^{(ji)}_{Elastic}$ is the elastic force exerted by a particle i on its neighbour j. The strain energy on a particle k is defined as:

$$U^{(k)} = \bar{v}^{(k)} \frac{1}{2} (\epsilon^{(k)}_{ij} \sigma^{(k)}_{ij}) \tag{4.12}$$

Using 4.12 in 4.11 we have the elastic force exerted by a particle k on its neighbour l:

$$\begin{aligned} F^{(lk)}_{Elastic} &= -\bar{v}^{(k)} \sigma^{(k)}_{ij} \nabla_{\mathbf{u}_l} \epsilon^{(k)}_{ij} \\ &= -2\bar{v}^{(i)} (I + \nabla \mathbf{u^{(i)}}^T) \sigma^{(i)} \mathbf{d^{(ij)}} \end{aligned} \tag{4.13}$$

Symmetrizing the elastic force according to [5] we have the elastic force on a particle i:

$$F^{(i)}_{Elastic} = \sum_j \frac{F^{(ij)}_{Elastic} - F^{(ji)}_{Elastic}}{2} \tag{4.14}$$

4.4 Pseudo Code to calculate elastic forces

```
1  force all particles Pi
2  {
3      initialise gradU with 0
4      for all body neighbours Pj of Pi
5      {
6          dij <- vBodyj gradW(xi-xj, h)
7          gradU <- gradU + dij(uj-ui)^T
8      }
9      epsilon <- 1/2(gradU + gradU^T + gradU*gradU^T)
10     sigma <- C_i epsilon
11     ElasticMatrix <- vBodyi (I + gradU^T)sigma
12     for all body neighbours Pj of Pi
13     {
14         halvedForce <- ElasticMatrix*dij
15         forceDensityj <- forceDensityj - halvedForce/vj
16         summedForce <- summedForce + halvedForce
17     }
18     forceDensityi <- forceDensityi + summedForce/vi
19 }
```

4.5 Sine Kernel

The kernel function used for the calculation of the elastic forces as suggested by [5].

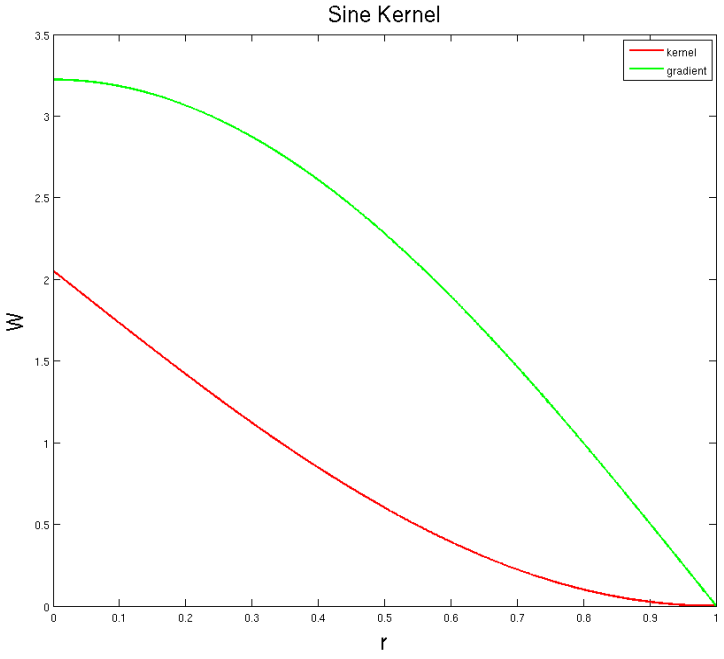

FIGURE 4.1: Sine Kernel

$$W_{sine}(\vec{r},h) = \begin{cases} c\frac{2h}{\pi}cos(\frac{(r+h)\pi}{2h}) + c\frac{2h}{\pi} & 0 \leq \vec{r} \leq h \\ 0 & otherwise \end{cases} \tag{4.15}$$

$$\nabla W_{sine}(\vec{r},h) = \begin{cases} -\frac{\vec{r}}{r}c.sin(\frac{(r+h)\pi}{2h}) & 0 \leq \vec{r} \leq h \\ 0 & otherwise \end{cases} \tag{4.16}$$

where c is a normalising factor.

$$c = \frac{\pi}{8h^4\left[\frac{\pi}{3} - \frac{8}{\pi} + \frac{16}{\pi^2}\right]} \tag{4.17}$$

Chapter 5

Implementation Environment

5.1 nVIDIA GTX 580 - GPU

Implementation of the Smoothed Particle Hydrodynamics code was done on a nVIDIA GTX - 580 GPU. OpenCL with a C++ wrapper was used for coding purposes. The below table shows the specification of the GPU used.

Name	GTX 580
Core clock [MHz]	1544
Multiprocessors	16
Cuda Cores	512
Memory[MB]	1536
Memory Bus[bit]	384
Memory clock[MHz]	2004
Maximum Memory Bandwidth(GB/s)	192.4
Host interface	PCIe 2.0 x16
Measured Memory Bandwidth SGEMV[MB/sec]	150.016
Measured Performance SGEMV[Mflops/sec]	74.89

The number of particles in a simulation in from 12 000 to 22 000 dependin on the simulation.

Chapter 6

Model of the Continuous Casting

6.1 Mold

The mold is a hollowed block that is filled with the molten metal. The hot molten metal cools and hardens inside the mold adopting its shape. To model this mold several columns of particles are used. The properties of these particles are that of copper. The outermost column is cooled which in turn cools the neighboring column until finally the hot fluid is cooled. The wall is kept oscillating. In the continuous casting the mold wall oscillates at a frequency of 1-2 Hz. An effort has been made in this simulation to incorporate this feature. 7.2 shows the oscillating wall.

6.1 shows the mold (turquoise particles) and the solidified shell (red particles) and the hot molten metal (blue particles)

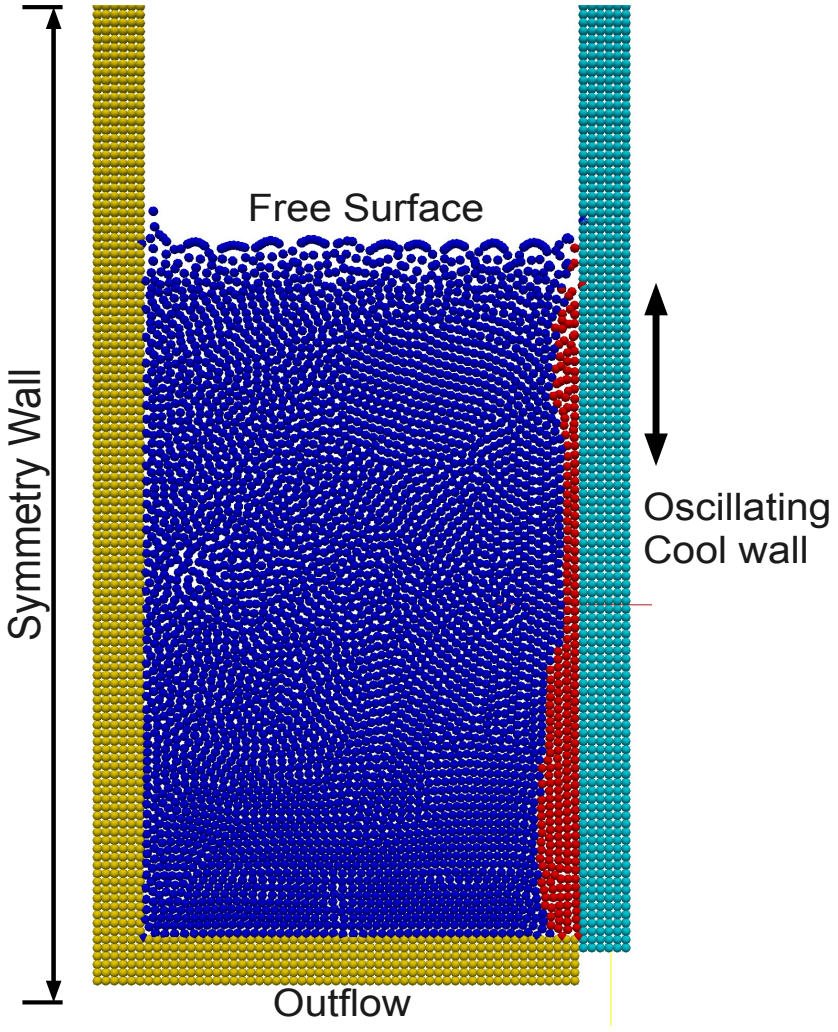

FIGURE 6.1: Mold represented by the turquoise particles

6.2 Submerged injection

6.2 shows the submerged injection jet. Molten metal from an overhead reservoir is injected at a constant rate depending on the outflow. Depending on the position of the inlet the shell thickness at that height is thin as the fluid heats up that part of the shell. The inflow is such that a steady state condition is reached where the outflow will be equal to the inflow and the level of the fluid remains constant. The number of particles per second that enters the mold(n_e) is equal to the number of particles leaving the mold(n_o). The mass flow rate is given by

$$\dot{m} = \rho \vec{v} A \tag{6.1}$$

where A is the area of cross section of the outlet and $\dot{m} = n_o * mass_{particle}$

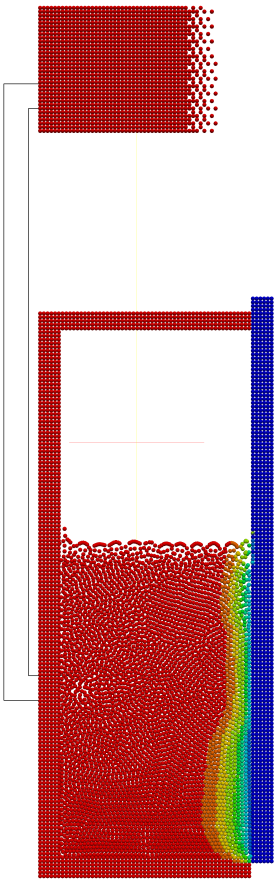

FIGURE 6.2: Inlet

6.3 Outflow

The velocity at which the particles leave is proportional to the pressure. To model this, either a friction band can be introduced or the velocity can be calculated and set to a value that is proportional to the pressure. Once a particle crosses the bottom boundary, it is returned to the reservoir. The outflow velocity is proportional to the pressure, i.e.

$$v = kp \tag{6.2}$$

The outlet velocity is known(around 1cm/s) and the value of k is calculated using the equilibrium height.

6.4 Water Spray

In continuous casting the molten metal solidifies forming a shell when it comes in contact with the cold wall. The mold of the continuous casting is modeled with a cold oscillating wall and a symmetric wall. Once the shell is formed water is sprayed on the solidified metal. If the shell is thin and cooling is not sufficient, the elastic body melts due to the effect of the hot fluid. The water is sprayed on the metal, absorbs the latent heat of vaporisation and evaporates.

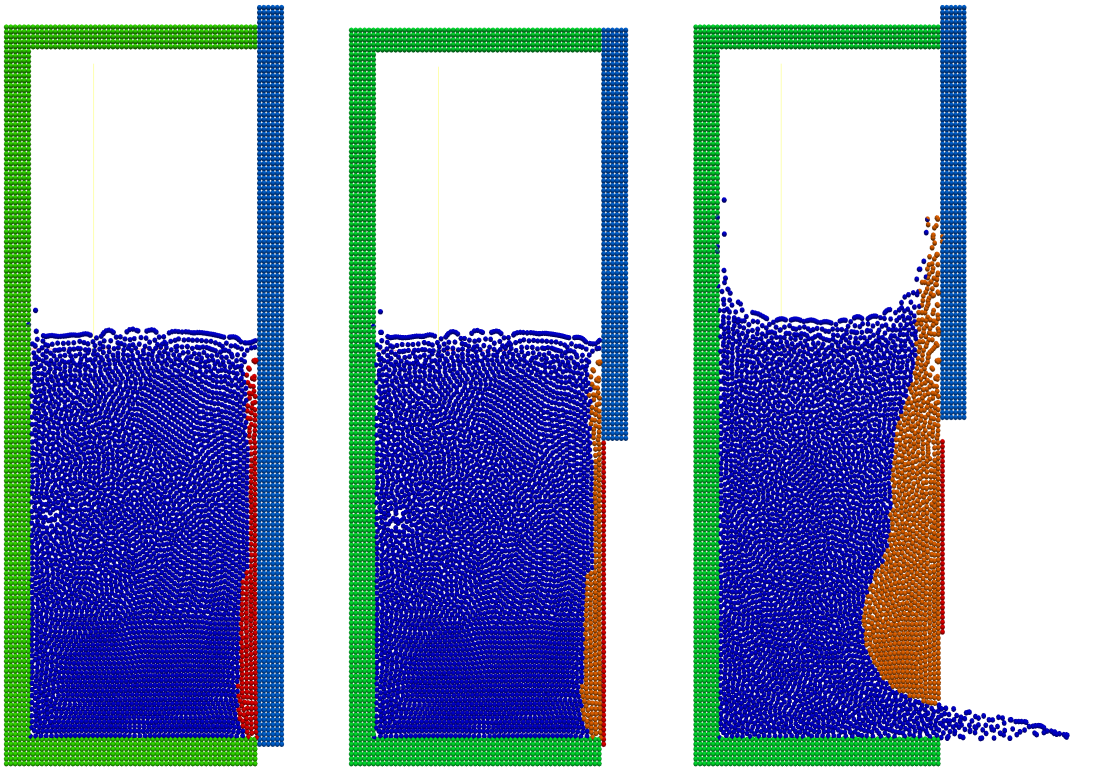

(a) t = 5s (Shell Formation)

(b) t = 10s (Shell cooled by water spray)

(c) t = 20s (No cooling at the bottom and shell breaks)

FIGURE 6.3: Water Spray

In 6.3 the red particles represents the water spray and the orange particles represents the solidified shell. The second figure shows that the water cooling is stopped in the bottom part of the mold, this makes the shell break/melt and the molten metal to flow out. In 3.2 the enthalpy depends on:

$$H \quad \alpha \quad \frac{\kappa_m \kappa_w}{\kappa_m + \kappa_w} \tag{6.3}$$

where κ_m and κ_w are thermal conductivities of metal and water respectively The thermal conductivity of water is kept very large so that the primary contribution is from the metal. A predetermined number of particles is sprayed on the metal per second. The enthalpy of the water increases, and when it reaches the enthalpy of vaporisation the water particle disappears. This is again replaced by another particle when water is sprayed again. In 6.3(a) the cooling is uniform and there is no breakage of the shell. Whereas in 6.3(c) the water spray is removed in the bottom part of the mold. This leads to the melting of the shell due to the action of the hot molten metal, and finally the shell gives way.

6.5 Dummy particles

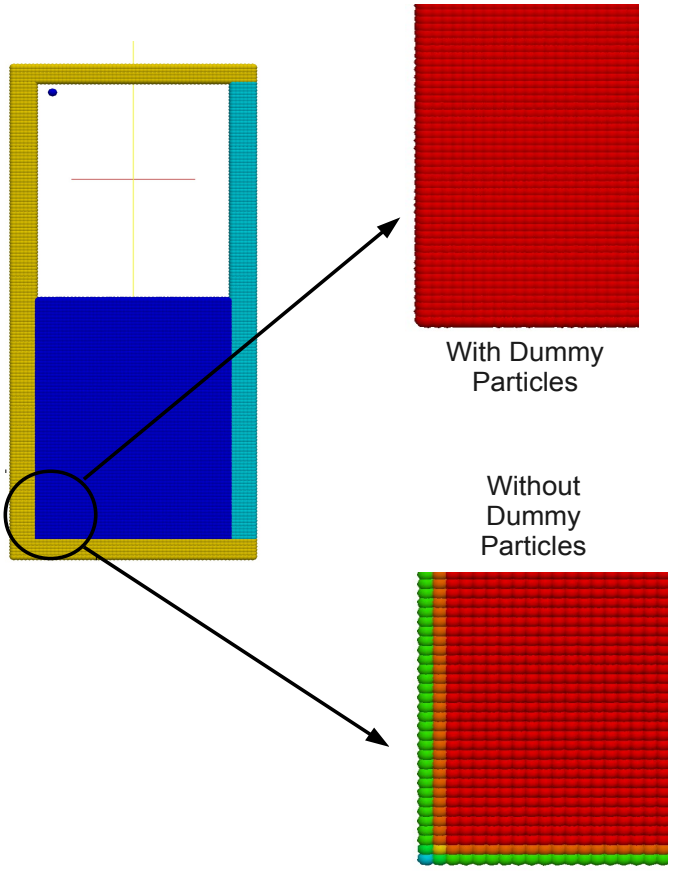

FIGURE 6.4: Mapping of Temperature from Enthalpy

The density of a particles is calculated by taking into account the particles surrounding it. In the boundary there are particles on only one side of the boundary particles. This results in undesired pressure waves, as there is a drastic change in density. This is

shown by 6.4 where we can see there is a change in density. To eliminate the pressure waves dummy particles are placed at the other side of the boundary particles, whose sole purpose is to eliminate the pressure waves by maintaining a constant density at the boundary. The yellow particles in 6.4 are the dummy particles. The properties of the dummy particles is same as that of the fluid steel particles. The positions of the dummy particles are not updated, and hence these are fixed. They are used only for calculation of density.

6.6 Initialization

The particles at the start of the simulation are placed in a regular grid 6.4. The temperature, mass, kinematic viscosity, initial density, speed of sound and velocities. The forces are calculated and the positions and velocities at the next time step is calculated.

In order to speed up the simulation the particles can be initially arranged based on hydrostatic pressure 6.5. This saves the time taken by the fluid to reach this configuration from the regular grid. When the velocity is zero 1.2 reduces to:

$$p_z = \rho g \tag{6.4}$$

with the boundary condition

$$p(h) = 0 \tag{6.5}$$

Where the right hand side represents the gravity and p is calculated using 1.5

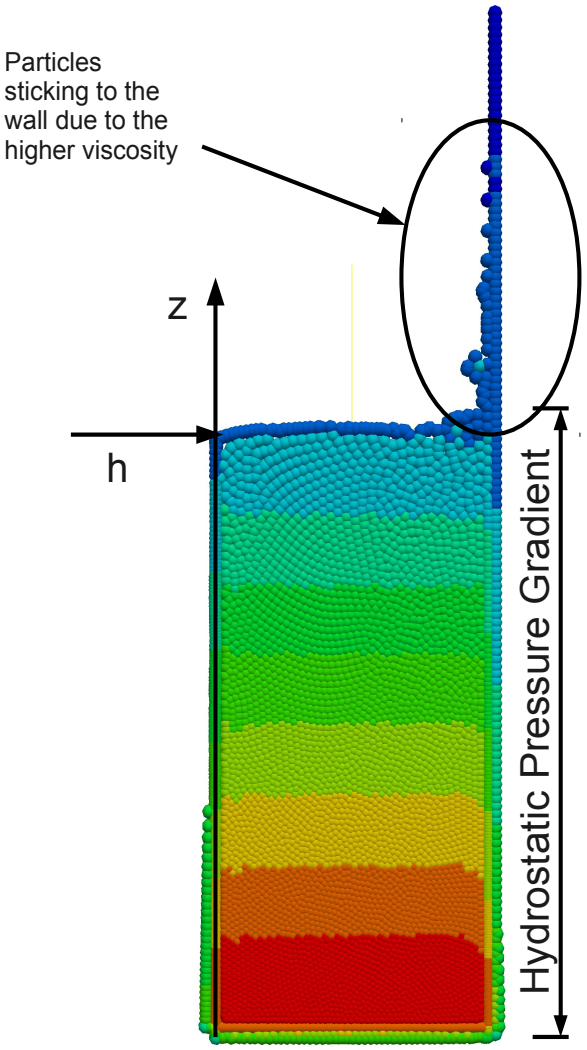

FIGURE 6.5: Particles arranged based on hydrostatic pressure

Chapter 7

Simulation Results

7.1 Validation of the Hydrostatic Pressure

The first step to have a correct simulation is to have the correct hydrostatic pressure values when the fluid has settled down. This is important as the shape and size of the shell depends on the pressure acting on it.

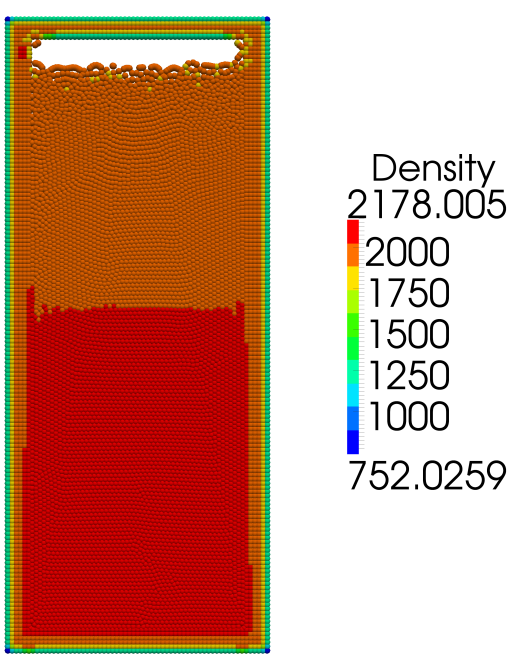

(a) Density

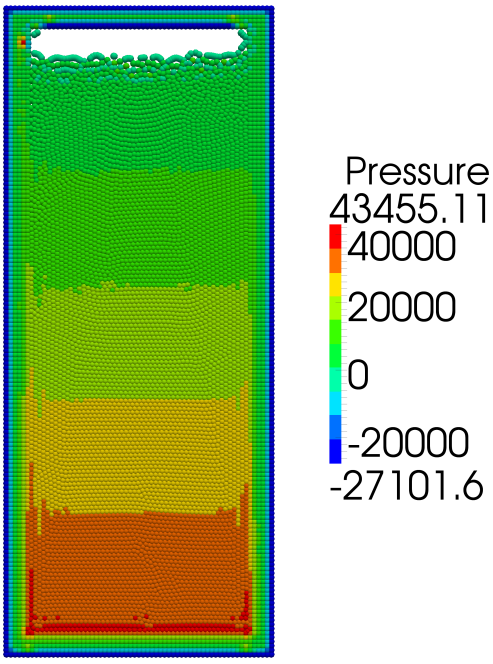

(b) Pressure

The length of the water column in 7.1(a) is 2.05m. The hydrostatic pressure is given by:

$$\begin{aligned} P &= \rho g h \\ &= 2178.005 * 9.81 * 2.05 \\ P &= 43800 kg/m^3 \end{aligned} \tag{7.1}$$

The above value of pressure at the bottom agrees with the value obtained from the simulation. Also we can see that there is only a slight variation of density (4%)

7.2 Formation of the shell

In continuous casting the molten metal solidifies forming a shell when it comes in contact with the cold wall. The thickness of the shell depends on the pressure exerted by the fluid on the shell, temperature of the fluid, the effectiveness of cooling. If the cooling is not proper, the thickness of the shell is less.

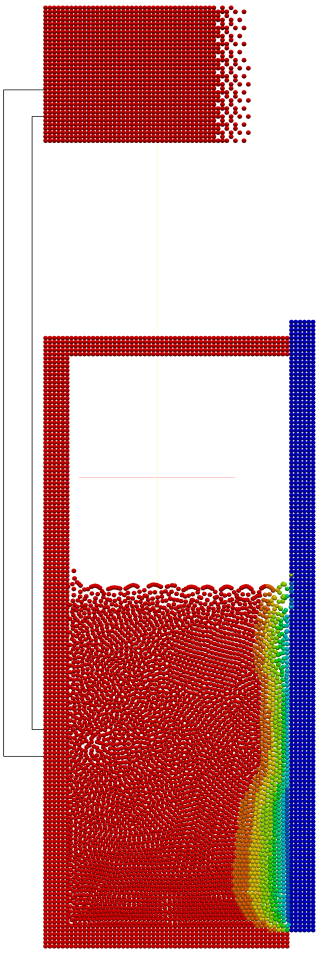

FIGURE 7.1: Effect of inlet position

7.7 shows the influence of inlet position on the thickness of the shell. Near the inlet the molten metal jet hits the shell and hence melting some of it. This leads to a thin shell thickness.

7.3 Oscillating Wall

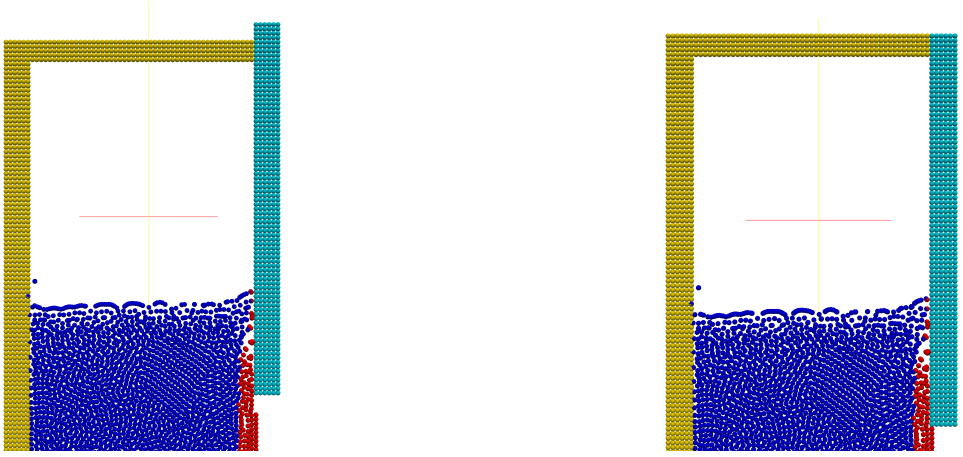

FIGURE 7.2: Oscillating Wall

Mold fluxes are used in steel continuous casting with the main objective of bringing adequate lubrication and heat extraction into the mold. Both parameters have decisive influence on both the surface quality and the structural characteristics required by different steels. This feature however has not been implemented in the simulation. With the oscillating wall one can expect a rim to be formed just above the surface, as some of the fluid particles are pulled by the wall and cools more faster. This cannot be seen in the simulation as the viscosity is not enough to develop the frictional force between the wall and the fluid.

7.4 Breaking of the shell

In this simulation an attempt has been made to simulate the effect of improper cooling water spray. Once the shell is formed it is cooled by water sprays. If one or more of this water sprays is malfunctioanl, the shell formed is damaged. This is because of the hot fluid melting the shell and also the forces on the shell due to the fluid particles. This leads to the weakening of the shell and if the cooling is non-existent then the entire

shell might break down. This simulation is particularly hard to do in Eulerian based approaches(COMSOL).

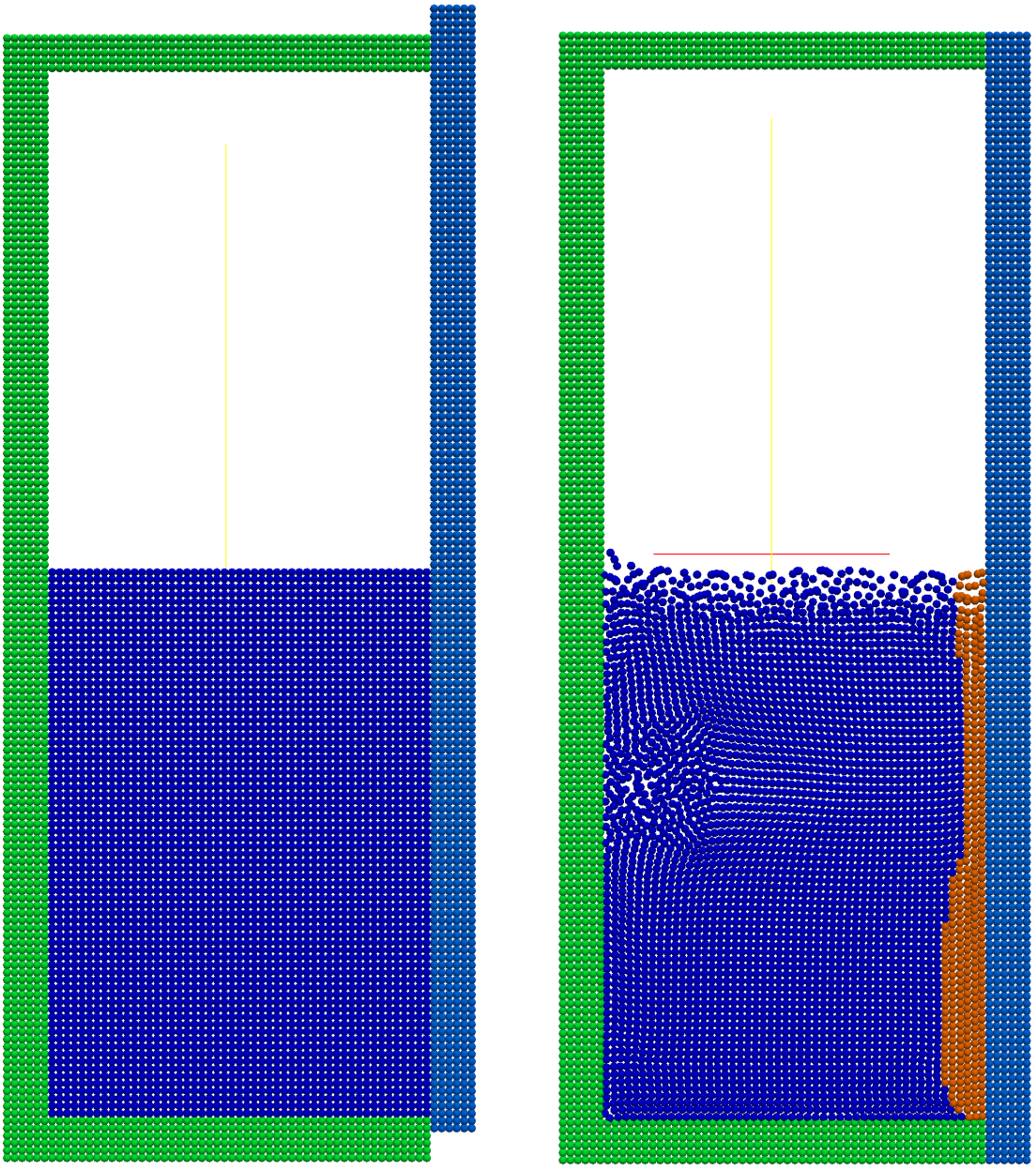

(a) Initial setting (t = 0)

(b) Formation of the shell (t = 4s)

FIGURE 7.3: Continuous casting simulation

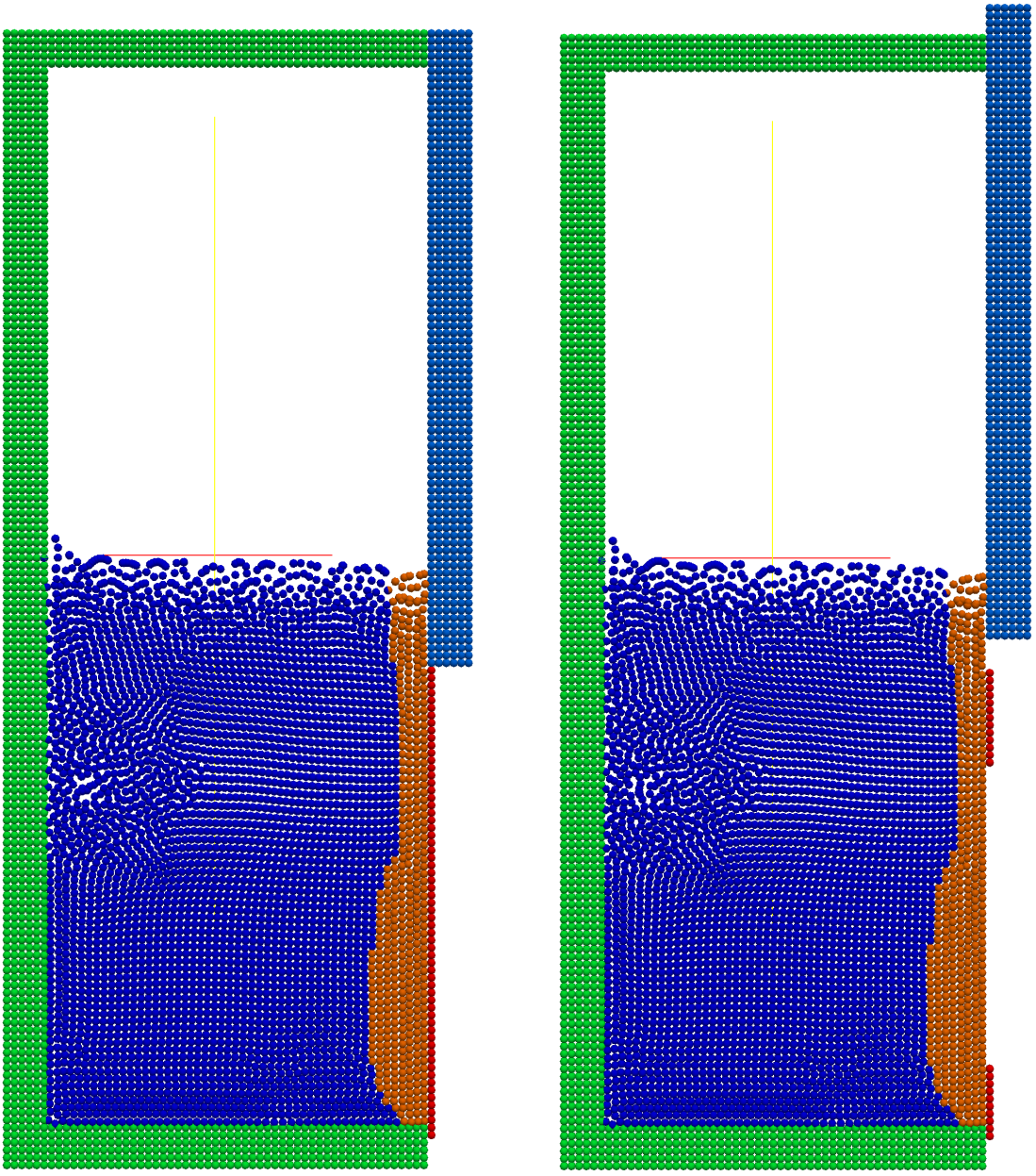

(a) Introduction of water spray (t = 6s)

(b) Removing part of the water spray (t = 8s)

FIGURE 7.4: Continuous casting simulation

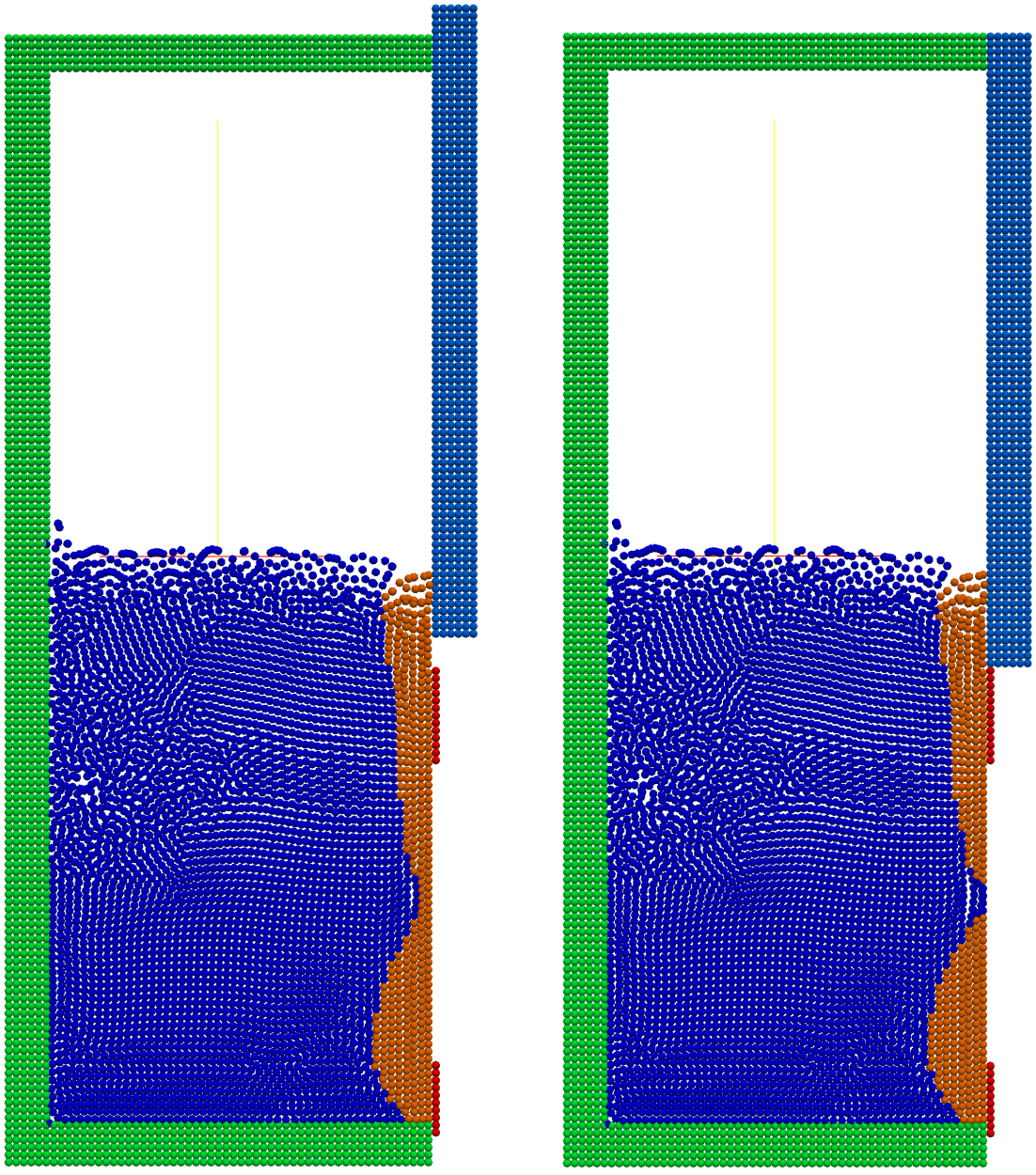

(a) Thinning of the shell where there is no cooling (t = 12s)

(b) Formation of a hole in the shell due to melting (t = 13s)

FIGURE 7.5: Continuous casting simulation

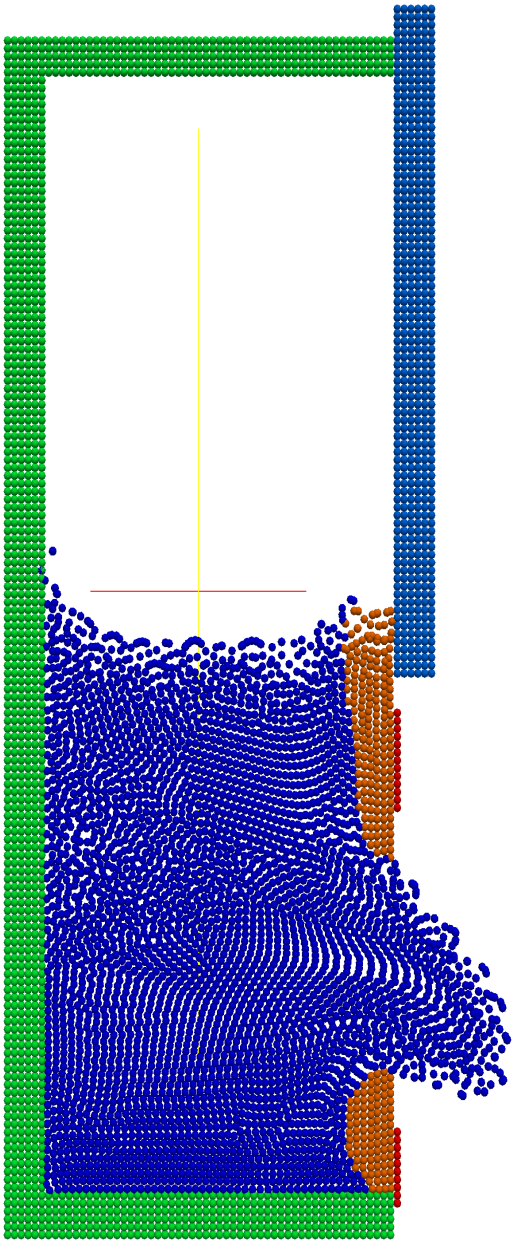

(a) Molten Metal Flowing from the hole (t = 15s)

FIGURE 7.6: Continuous casting simulation

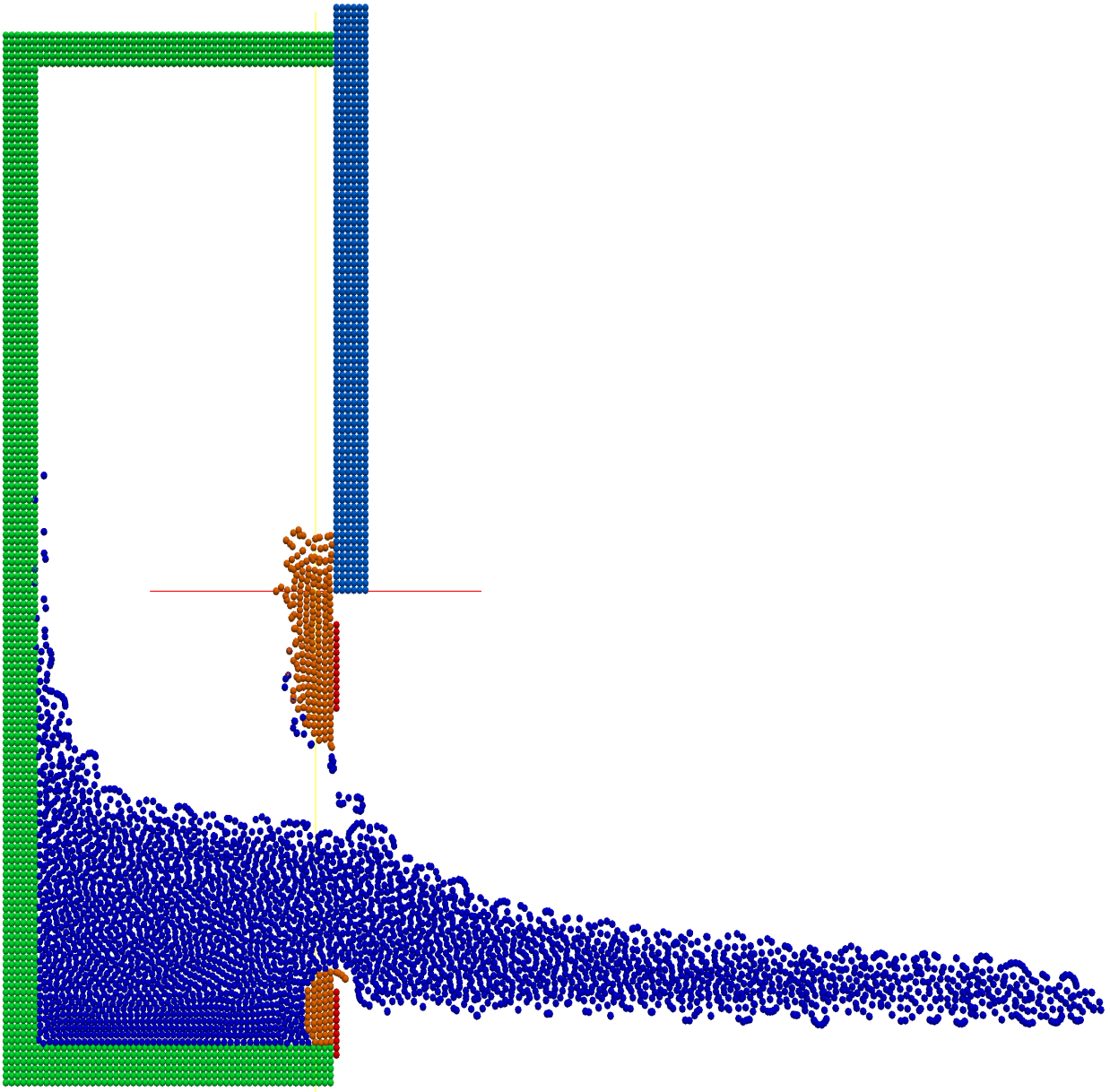

FIGURE 7.7: Molten Metal Flowing from the hole (t = 18s)

7.5 Simulation Parameters

7.5.1 Fluid Volume, Particle Mass and Density

The number of particles in a fluid (n) of volume V(m^3) is given by:

$$n = \rho \frac{V}{m} \tag{7.2}$$

where ρ is the density of the fluid (kg/m^3) and m is the mass of each particle (kg). The density of steel is about $7800 kg/m^3$. In our simulation we were able to achieve only a density of 2100 kg/m^3. This is because in order to increase the density the mass of each pparticle has to be increased. If the mass is increased then the viscosity will not provide suffcient damping. Hence the viscosity must be increased by orders of magnitude than the actual value of steel.

7.5.2 Smoothing Kernel Support Radius

The support radius plays a very important role in stability and robustness of the simulation. The support radius mus neither be too large nor too small. A very large support radius(h) gives inaccurate answers as the kernel weights particles near the centre less than when h is small. If h$\rightarrow$0, this also produces an inaccurate result as the number of particles are too less. The number of particles in the support radius in 3D can be calculated as:

$$\begin{aligned} x &= \frac{n}{V}\frac{4}{3}\pi h^3 \\ h &= \sqrt[3]{\frac{3vx}{4\pi n}} \end{aligned} \tag{7.3}$$

x should be chosen to be the smallest possible amount of particles that renders the fluid simulation stable, while still respecting the properties of the fluid material.

7.5.3 Speed of sound

The Mach number M is given by :

$$M = v_{casting}/c_s \tag{7.4}$$

where $v_{casting}$ is the average speed of particles in the casting and c_s is the speed of sound. The speed of sound in the simulation is taken as 10 and $v_{casting} = 0.01$. This leads to a Mach number of 0.001. We know that

$$M^2 = 2\frac{\delta\rho}{\rho} \tag{7.5}$$

A Mach number value of 0.001 leads to a density variation in percentage.

7.5.4 Co-efficient of Viscosity

The viscous force physically simulates the viscous behaviour fluis and numerically it makes the system more dissipative. In this simulation to have a resonable damping the value of viscosity co-efficient must be atleast 1000 times larger than the actual value.

7.5.5 Time Step

The time step is limited for the momentum and for the energy equation as suggested by [6]. The timestep for explicit integration is limited by the Courant condition modified for the presence of viscosity:

$$\Delta t = min_a \left[\frac{0.5h}{c_s + \frac{2\xi\mu_a}{h\rho_a}} \right] \tag{7.6}$$

where h is the supprot radius, ρ_a is the density of particle a, μ is the viscosity co-efficient and $\xi = 4.9633$

The maximum timestep for the explicit integration of the energy equation is :

$$\Delta t = \zeta\rho c_v h^2/k \tag{7.7}$$

where ζ is found to be 0.1.

Bibliography

[1] J.J Monaghan. Smoothed particle hydrodynamics. *Annual Review of Astronomy and Astrophysics*, 30:543–574, 1992.

[2] M. Müller, D. Charypar, and M. Gross. Particle-based fluid simulation for interactive applications. *Proceedings of 2003 ACM SIGGRAPH Symposium on Computer Animation*, pages 154–159, 2003.

[3] P. Cleary et al. Effect of heat transfer and solidification on high pressure die casting. *Monash University*, pages 697–682, 1998.

[4] R. Keiser, B. Adams, D. Gasser, P. Bazzi, P. Dutré, and M. Gross. Unified lagrangian approach to solid-fluid animation. *In Proceedings of the Eurographics Symposium on Point- Based Graphics*, pages 125–133, 2005.

[5] M. Muller, R. Keiser, A. Nealen, M. Pauly, M. Gross, and M. Alexa. Point based animation of elastic, plastic and melting objects. *In Proceedings of the 2004 ACM SIGGRAPH/Eurographics Symposium on Computer Animation*, pages 141–151, 2004.

[6] Paul. W. Cleary. Modeling confined multi-material heat and mass flows using sph. *CSIRO Division of Mathematical and information sciences, Clayton, Victoria.*

TRITA-MAT-E 2012:11
ISRN-KTH/MAT/E--12/11-SE

www.kth.se